Copy 193
RM A54H12a

RESEARCH MEMORANDUM

THE EFFECT OF WING PROFILE ON THE TRANSONIC CHARACTERISTICS OF RECTANGULAR AND TRIANGULAR WINGS HAVING ASPECT RATIOS OF 3 - TRANSONIC BUMP TECHNIQUE

By Warren H. Nelson and Joseph L. Frank

Ames Aeronautical Laboratory
Moffett Field, Calif.

NATIONAL ADVISORY COMMITTEE
FOR AERONAUTICS
WASHINGTON
October 27, 1954

NATIONAL ADVISORY COMMITTEE FOR AERONAUTICS

RESEARCH MEMORANDUM

THE EFFECT OF WING PROFILE ON THE TRANSONIC CHARACTERISTICS OF RECTANGULAR AND TRIANGULAR WINGS HAVING ASPECT RATIOS OF 3 - TRANSONIC BUMP TECHNIQUE

By Warren H. Nelson and Joseph L. Frank

SUMMARY

An investigation was conducted to determine the effect of wing profile on the transonic aerodynamic characteristics of rectangular and triangular wings having aspect ratios of 3. The characteristics of five wings, three rectangular and two triangular, were compared. The rectangular wings utilized 4-percent-thick, circular-arc, NACA 2-004, and NACA 63A004 profiles, and the triangular wings utilized NACA 2-004 and NACA 63A004 profiles. The Mach number range of the tests, in general, was 0.6 to 1.10, corresponding to a Reynolds number range of 1.7 million to 2.8 million.

For both the triangular and rectangular wings, these variations in profile had no major effect on the transonic characteristics, however, in the case of the triangular wings, the wing having the NACA 2-004 profile had a lower drag-rise parameter below 0.9 Mach number.

INTRODUCTION

A program of systematic research has been in progress in the Ames 16-foot high-speed wind tunnel to determine the aerodynamic characteristics of various wings through the transonic speed range utilizing the bump technique. The over-all program to date has included investigations to determine the effects of aspect ratio, thickness ratio, camber, planform taper ratio, and spanwise variations in thickness ratio of rectangular wings. In addition, the effects of aspect ratio, thickness ratio, and wing-tip clipping have been investigated for triangular wings. The results of all these investigations are presented in references 1 through 8.

The purpose of this report is to present that part of the general program concerning the effects of wing profile on the aerodynamic characteristics of rectangular and triangular wings having aspect ratios of 3. The three sections used in this investigation were selected to provide large variations in profile; they were the NACA 2-004 section with its relatively blunt leading edge, the NACA 63A004 section, which has been used throughout the general research program, and the 4-percent-thick, circular-arc section with a sharp leading edge.

NOTATION

C_D drag coefficient, $\frac{\text{twice semispan drag}}{qS}$

C_{D_o} minimum drag coefficient

C_{D_f} friction-drag coefficient, assumed equal to the minimum drag coefficient at a Mach number of 0.7

$(C_{D_P})_{min}$ minimum pressure-drag coefficient, assumed equal to $C_{D_o} - C_{D_f}$

C_L lift coefficient, $\frac{\text{twice semispan lift}}{qS}$

C_m pitching-moment coefficient, referred to $0.25\bar{c}$, $\frac{\text{twice semispan pitching moment}}{qS\bar{c}}$

M mean Mach number in region of wing

M_L local Mach number

S total wing area, twice area of semispan model, sq ft

S_c total cross-sectional area, twice cross-sectional area of semispan model, sq ft

V velocity, ft/sec

b twice span of semispan model, ft

c local wing chord, ft

$\bar{c}$ mean aerodynamic chord, $\frac{\int_o^{b/2} c^2 dy}{\int_o^{b/2} c\, dy}$, ft

q dynamic pressure in region of wing, $\frac{1}{2}\rho V^2$, lb/sq ft

x	chordwise distance from leading edge, ft
y	spanwise distance from plane of symmetry, ft
α	angle of attack, deg
ρ	air density in region of wing, slugs/cu ft

APPARATUS AND MODELS

The tests were conducted in the Ames 16-foot high-speed wind tunnel utilizing a transonic bump. A description of the transonic bump is given in reference 9. The forces and moments were measured by means of a strain-gage balance mounted within the bump.

A photograph of one of the models is shown in figure 1, and sketches of typical models are shown in figure 2. Three wings, one triangular and two rectangular, having aspect ratios of 3, were constructed of steel. The rectangular wings utilized circular-arc and NACA 2-004 profiles, and the triangular wing had an NACA 2-004 profile. Sketches of the three profiles used are shown in figure 3 and the coordinates are given in table I. The ordinates for the NACA 63A004 and NACA 2-004 profiles were proportionately reduced from ordinates for 6-percent-thick profiles. The tips of the rectangular wings were semibodies of revolution developed by rotating the tip sections.

A fence, attached to the support at the wing root 3/16 inch from the bump surface, was used to prevent the flow through the gap, between the wing and the bump surface, from affecting the flow over the wing.

TESTS AND PROCEDURE

Lift, drag, and pitching-moment data were obtained for the wings over a Mach number range of 0.6 to 1.10. For this Mach number range the Reynolds number, under the test conditions, varied from 1.7 million to 2.1 million for the rectangular wings, and from 2.2 million to 2.8 million for the triangular wings. In general, the angle of attack was varied from -2° to the angle for stall or to the angle where the root bending stress became critical.

A Mach number gradient existed in the flow over the bump where the wings were mounted. Typical contours of the local Mach number over the bump in the absence of the wings are shown in figure 4. Outlines of the rectangular and triangular wings have been superimposed on the contours to indicate the Mach number gradients which existed over the wings during

[redacted]

the tests. No attempt has been made to evaluate the effects of these gradients. The test Mach numbers presented are the mean values over the wings.

The data have been reduced to standard NACA coefficients. A tare correction to the drag was made to account for the drag of the fence and support. This drag tare was evaluated by cutting the wing off flush with the fence and measuring the forces on the fence and support. The mutual interference effects between the fence and the wings and the effects of leakage around the fence are unknown.

RESULTS AND DISCUSSION

Summary curves of the lift, drag, and pitching-moment data for the wings are presented in figures 5 through 8. Chordwise distribution of cross-sectional areas and minimum-pressure drags for the wings (as defined under NOTATION) are shown in figure 9. The lift, drag, and pitching-moment data for the wings of the present tests are presented in figures 10 through 12. The lift, drag, and pitching-moment data for the rectangular wing having the NACA 63A004 section, which were obtained for the investigation reported in reference 2, are shown in figure 13. The slopes $dC_L/d\alpha$ and dC_m/dC_L given in the summary figures were determined through zero lift, except those for the rectangular wing having a circular-arc profile. For this wing, the slopes were taken at a lift coefficient of 0.1, since the sudden change in slope through zero lift at subsonic speeds was not considered typical of the slope at slightly higher or lower lift coefficients.

The discussion is divided into three parts, the first dealing with the rectangular wings, the second dealing with the triangular wings, and the third dealing with transonic-area-rule considerations.

Rectangular Wings

The minimum drag coefficients for the rectangular wings are shown in figure 5. The wing having the NACA 63A004 profile had the lowest minimum drag throughout the Mach number range. The minimum drag coefficient for the wing having the NACA 2-004 profile increased as the Mach number was increased from 0.6 to 0.8, as opposed to essentially no change for the other wings. A drag increase similar to that for the NACA 2-004 wing has been observed at higher Reynolds numbers on a 45° swept wing having an NACA 2-006 profile (ref. 10). An explanation of the drag rise probably lies in a flow phenomenon of the boundary layer rather than an effect of compressibility, since the critical Mach number for this section is approximately 0.79.

The minimum pressure-drag coefficients as functions of Mach number are shown in figure 5. The minimum pressure-drag coefficient was calculated by subtracting from the total minimum drag coefficient a friction-drag coefficient, which was assumed equal to the minimum drag coefficient at 0.7 Mach number. The minimum pressure-drag coefficients for the NACA 63A004 and circular-arc wings were approximately the same, and they were less than those for the NACA 2-004 wing throughout the Mach number range. The peak pressure drag for the NACA 2-004 wing was about 35 percent greater than that for the NACA 63A004 wing.

The drag-rise parameter (dC_D/dC_L^2) for the wings, determined over a lift coefficient range of 0 to 0.3, is shown in figure 5. The NACA 2-004 wing had the lowest drag-rise factor up to 0.8 Mach number, and the circular-arc wing had the highest. These differences at low speed are attributed to the differences in leading-edge suction which, in turn, are a function of leading-edge radius. The difference in leading-edge radii becomes more apparent when it is realized that the leading-edge radius of an NACA 2-004 profile is three times as large as that for an NACA 63A004 profile and is equivalent to that for an NACA 63A007 profile. The drag-rise parameter for the NACA 2-004 wing increased rapidly above 0.75 Mach number, so that at 0.825 Mach number it was about the same as for the other wings. The sudden increase is probably the result of adverse compressibility effects on the flow in the region of the relatively thick leading edge. Above 0.825 Mach number, the difference in drag-rise parameter for the wings was small. This maximum difference in terms of drag coefficient amounted to 0.0010 at a lift coefficient of 0.2.

The lift-curve slopes for the rectangular wings are shown in figure 6. The slopes for the NACA 2-004 and NACA 63A004 wings were essentially identical throughout the Mach number range. The lift-curve slopes for the circular-arc wing above 0.80 Mach number were lower than those of the other wings. This is probably a result of separation occurring over the after portion of the wing at low angles of attack. Such separation on a 10-percent-thick circular-arc section was discussed in reference 11.

When the maximum lift coefficients of the wings are compared at the Mach numbers where maximum lift was attained, as shown in figures 10(a), 11, and 13(a), it is apparent they were approximately the same. This is in contrast to the data of reference 12, where tests at low speed of a wing having an infinite aspect ratio and an NACA 2-006 profile indicated a gain in maximum lift coefficient of 0.5 over the wing with 6-series sections. However, the Reynolds numbers of the present tests were low, possibly preventing a fair comparison of the maximum-lift data.

The pitching-moment-curve slopes for the wings are shown in figure 6. The over-all change in pitching-moment-curve slope in going from subsonic to supersonic speeds was greatest for the NACA 63A004 and NACA 2-004 wings, amounting to about three times that of the circular-arc wing. This large

change in pitching-moment-curve slope becomes important in performance comparisons when the increase in drag due to trim is considered.

Triangular Wings

The minimum drag coefficients for the two triangular wings are shown in figure 7. Again, as was the case for the rectangular wing, the minimum drag coefficient for the wing having the NACA 2-004 profile increased at subcritical Mach numbers. However, the differences in the minimum drags were small throughout the Mach number range, the maximum difference being approximately 0.0015 above a Mach number of 0.80.

The minimum pressure-drag coefficients for the triangular wings are shown in figure 7. The friction-drag coefficient used in calculating the minimum pressure-drag coefficient was assumed to be equal to the minimum drag coefficient at 0.70 Mach number, and was the same for both wings. On this basis, the NACA 2-004 wing had a slightly higher pressure drag above 0.70 Mach number. However, if the friction-drag coefficient had been taken as the minimum drag coefficient at some Mach number only slightly below the drag-divergence Mach number, the pressure drags would have been essentially the same for the wings.

The drag-rise parameters for the wings are shown in figure 7. The NACA 2-004 wing had the lowest drag-rise parameter throughout the Mach number range. However, in the transonic speed range there was little difference between the wings. The maximum difference at transonic speeds in terms of drag coefficient amounted to only 0.0010 at a lift coefficient of 0.2. The large difference in drag-rise parameter below 0.8 Mach number is probably a result of the more favorable suction conditions at the leading edge of the NACA 2-004 wing, due to the relatively large leading-edge radius. Above 0.8 Mach number, the rapid increase in drag-rise parameter for the NACA 2-004 wing is probably a result of compressibility effects becoming more prominent and influencing the type of flow over the nose. Above 0.95 Mach number, the magnitudes and variations of the drag-rise parameter are approximated by the reciprocal of the lift-curve slopes, indicating that the leading-edge suction for these Mach numbers had decreased to essentially zero. A large effect of Reynolds number on drag-rise parameter has been shown in reference 13; accordingly, the drag-rise data in this report should be used with caution.

The lift-curve slopes as a function of Mach number for the two triangular wings are shown in figure 8. The lift-curve slopes were approximately equal throughout the Mach number range, although the peak value occurred at a slightly higher Mach number for the NACA 2-004 wing. A comparison of the NACA 2-004 wing and the NACA 63A004 wing (fig. 12(a) and ref. 6) on the basis of maximum lift indicates essentially no

difference for the Mach number range over which maximum lift was attained. This was also true for the rectangular wings as was mentioned previously.

The pitching-moment-curve slopes as a function of Mach number are shown in figure 8. The maximum over-all change in pitching-moment-curve slope over the Mach number range of the tests for the NACA 63A004 wing was approximately one-third greater than that for the NACA 2-004 wing. This difference in pitching-moment-curve slope becomes important when, other conditions being the same, the drag is considered in the light of trim conditions.

Transonic Area Rule

The concepts of the transonic area rule which have been presented in reference 14 are, in effect, that near the speed of sound, the zero-lift drag rise of a thin low-aspect-ratio wing-body combination is primarily dependent on the axial variation of cross-sectional areas normal to the air stream. The analysis of the available drag-rise data mentioned in reference 14 indicated that variations in wing configuration which resulted in less rapid rates of development of cross-sectional area, as well as reductions of the relative magnitude of the maximum areas, decreased the drag-rise increments near the speed of sound. The data of the present investigation will be discussed in light of the transonic area rule.

The chordwise variations of cross-sectional areas and the minimum pressure-drag coefficients for the wings are shown in figure 9. Of the three rectangular wings, the NACA 2-004 wing would be expected to have the greatest pressure-drag rise near a Mach number of 1.0 on the basis of a greater rate of cross-sectional-area increase. This was the case as shown in figure 9.

It is apparent that the maximum cross-sectional areas of the triangular wings were smaller with respect to the wing area than those of the rectangular wings and, as the area rule would indicate, the pressure-drag rises were also lower. The triangular wing with the NACA 2-004 profile would be expected to have a lower pressure-drag rise than the triangular wing with the NACA 63A004 profile since it had a smaller maximum cross-sectional area and a more symmetrical distribution. Theoretical pressure-drag rises at a Mach number of 1.0 were calculated according to the methods of reference 15, and these calculations indicate a pressure-drag rise for the NACA 2-004 wing equal to one-half that for the NACA 63A004 wing. However, the pressure-drag rise for the NACA 2-004 wing was greatest (fig. 9). (If the pressure drags had been taken as the increment above the drag values at 0.85 or 0.9 Mach number, the pressure-drag rise would have been the same for both wings.) It is apparent, then, that the difference in pressure-drag rise predicted by the area rule was

not realized experimentally. This discrepancy between experiment and the area rule could represent a shortcoming of the area rule and is probably indicative of the importance of local or secondary effects. In this case, it is believed, the flow over the wing was affected by the relatively blunt leading edge to such an extent that an adverse increase in pressure drag occurred. It is interesting to note that an attempt has been made in reference 16 to establish a limit to the range of wing configurations to which the transonic area rule is applicable. The analysis was made on the basis of data presented for rectangular wings in references 2 and 6.

CONCLUDING REMARK

The results of these tests indicate no major effects of profile on the transonic aerodynamic characteristics of rectangular and triangular wings of aspect ratio 3, however, for the triangular wings, the wing having an NACA 2-004 profile had a lower drag-rise parameter below 0.9 Mach number.

Ames Aeronautical Laboratory
National Advisory Committee for Aeronautics
Moffett, Field, Calif., Aug. 12, 1954

REFERENCES

1. Nelson, Warren H., and McDevitt, John B.: The Transonic Characteristics of 17 Rectangular, Symmetrical Wing Models of Varying Aspect Ratio and Thickness. NACA RM A51A12, 1951.

2. McDevitt, John B.: A Correlation by Means of the Transonic Similarity Rules of the Experimentally Determined Characteristics of 22 Rectangular Wings of Symmetrical Profile. NACA RM A51L17b, 1952.

3. Nelson, Warren H., and Krumm, Walter J.: The Transonic Characteristics of 38 Cambered Rectangular Wings of Varying Aspect Ratio and Thickness as Determined by the Transonic Bump Technique. NACA RM A52D11, 1952.

4. McDevitt, John B.: A Correlation by Means of Transonic Similarity Rules of the Experimentally Determined Characteristics of 18 Cambered Wings of Rectangular Plan Form. NACA RM A53G31, 1953.

5. Nelson, Warren H., Allen, Edwin C., and Krumm, Walter J.: The Transonic Characteristics of 36 Symmetrical Wings of Varying Taper, Aspect Ratio, and Thickness as Determined by the Transonic-Bump Technique. NACA RM A53I29, 1953.

6. Emerson, Horace F.: Wing-Tunnel Investigation of the Effect of Clipping the Tips of Triangular Wings of Different Thickness, Camber, and Aspect Ratio - Transonic Bump Method. NACA RM A53L03, 1954.

7. Nelson, Warren H.: The Transonic Characteristics of Unswept Wings Having Aspect Ratios of 4, Spanwise Variations in Thickness Ratio, and Variations in Plan-Form Taper - Transonic-Bump Technique. NACA RM A53L17, 1954.

8. Cleary, Joseph W.: The Transonic Aerodynamic Characteristics of Structurally Related Wings of Low Aspect Ratio Having a Spanwise Variation in Thickness Ratio - Transonic Bump Technique. NACA RM A54B18, 1954.

9. Axelson, John A., and Taylor, Robert A.: Preliminary Investigation of the Transonic Characteristics of an NACA Submerged Inlet. NACA RM A50C13, 1950.

10. Racisz, Stanley F., and Paradiso, Nicholas J.: Wind-Tunnel Investigation at High and Low Subsonic Mach Numbers of a Thin Sweptback Wing Having an Airfoil Section Designed for High Maximum Lift. NACA RM L51L04, 1952.

11. Summers, James L., and Page, William A.: Lift and Moment Characteristics at Subsonic Mach Numbers of Four 10-Percent-Thick Airfoil Sections of Varying Trailing-Edge Thickness. NACA RM A50J09, 1950.

12. Loftin, Laurence K., Jr., and Von Doenhoff, Albert E.: Exploratory Investigation at High and Low Subsonic Mach Numbers of Two Experimental 6-Percent-Thick Airfoil Sections Designed to Have High Maximum Lift Coefficients. NACA RM L51F06, 1951.

13. Osborne, Robert S., and Kelly, Thomas C.: A Note on the Drag Due to Lift of Delta Wings at Mach Numbers Up to 2.0. NACA RM L53A16a, 1953.

14. Whitcomb, Richard T.: A Study of the Zero-Lift Drag-Rise Characteristics of Wing-Body Combinations Near the Speed of Sound. NACA RM L52H08, 1952.

15. Holdaway, George H.: Comparison of Theoretical and Experimental Zero-Lift Drag-Rise Characteristics of Wing-Body-Tail Combinations Near the Speed of Sound. NACA RM A53H17, 1953.

[redacted]

16. Spreiter, John R.: On the Range of Applicability of the Transonic Area Rule. NACA RM A54F28, 1954.

TABLE I.- COORDINATES FOR THE PROFILES USED

[Stations and ordinates in percent airfoil chord]

NACA 2-004 profile		
Station	Upper-surface ordinate	Lower-surface ordinate
0	0	0
.501	.625	-.625
2.008	1.179	-1.179
4.541	1.609	-1.609
8.114	1.879	-1.879
12.717	1.989	-1.989
18.292	1.975	-1.975
24.727	1.873	-1.873
31.828	1.707	-1.707
35.00	1.628	-1.628
40.00	1.503	-1.503
45.00	1.377	-1.377
50.00	1.252	-1.252
55.00	1.127	-1.127
60.00	1.002	-1.002
65.00	.877	-.877
70.00	.751	-.751
75.00	.626	-.626
80.00	.501	-.501
85.00	.376	-.376
90.00	.251	-.251
95.00	.125	-.125
100.00	0	0
L.E. radius = 0.358		

NACA 63A004 profile		
Station	Upper-surface ordinate	Lower-surface ordinate
0	0	0
.5	.330	-.330
.75	.397	-.397
1.25	.503	-.503
2.50	.697	-.697
5.00	.965	-.965
7.50	1.165	-1.165
10.00	1.326	-1.326
15.00	1.575	-1.575
20.00	1.754	-1.754
25.00	1.880	-1.880
30.00	1.961	-1.961
35.00	1.997	-1.997
40.00	1.990	-1.990
45.00	1.943	-1.943
50.00	1.859	-1.859
55.00	1.742	-1.742
60.00	1.597	-1.597
65.00	1.429	-1.429
70.00	1.239	-1.239
75.00	1.037	-1.037
80.00	.832	-.832
85.00	.626	-.626
90.00	.420	-.420
95.00	.215	-.215
100.00	.009	-.009
L.E. radius = 0.118		

4-percent-thick circular-arc profile		
Station	Upper-surface ordinate	Lower-surface ordinate
0	0	0
1.25	.099	-.099
2.50	.195	-.195
5.00	.380	-.380
7.50	.556	-.556
10.00	.721	-.721
15.00	1.021	-1.021
20.00	1.281	-1.281
25.00	1.501	-1.501
30.00	1.680	-1.680
40.00	1.920	-1.920
50.00	2.000	-2.000
60.00	1.920	-1.920
70.00	1.680	-1.680
80.00	1.281	-1.281
90.00	.721	-.721
100.00	0	0

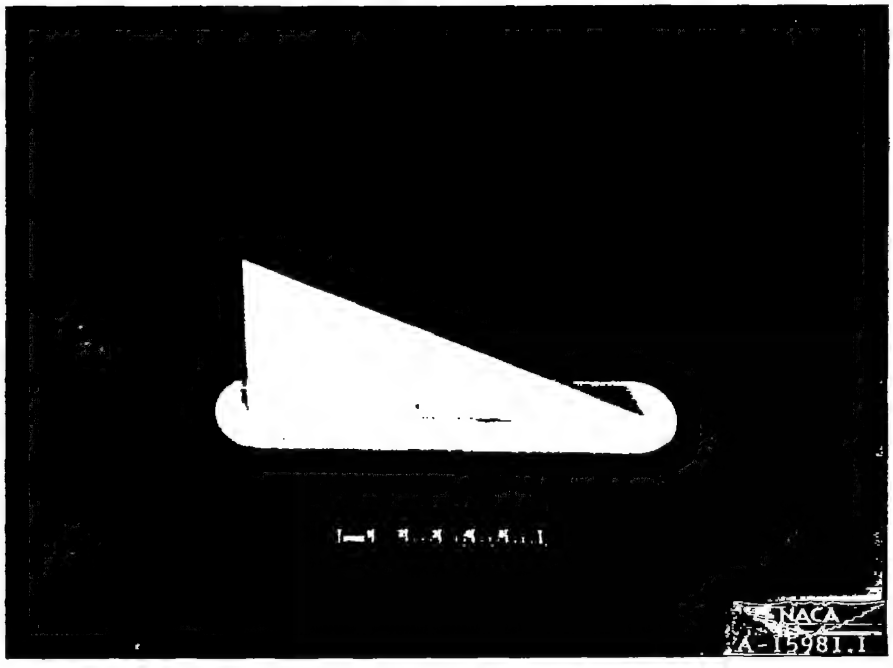

Figure 1.- A triangular wing having an aspect ratio of 3 mounted on the bump.

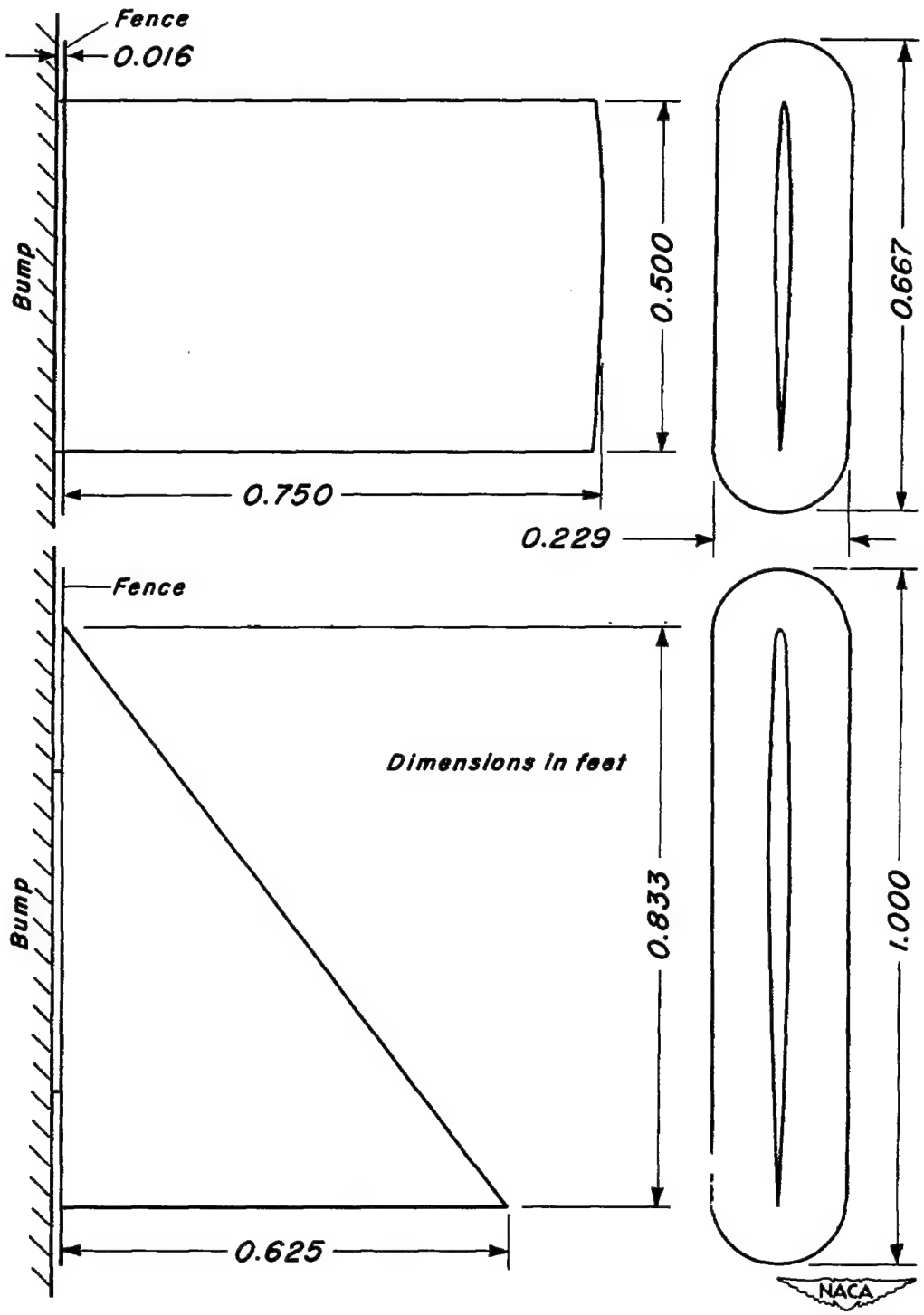

Figure 2.- Sketches of typical models.

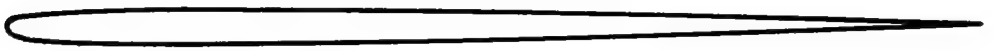

NACA 2-004

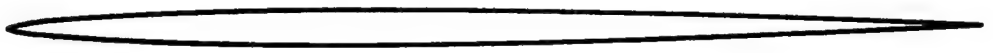

NACA 63A004

Circular arc

Figure 3.- Sketches of the profiles used for the wings.

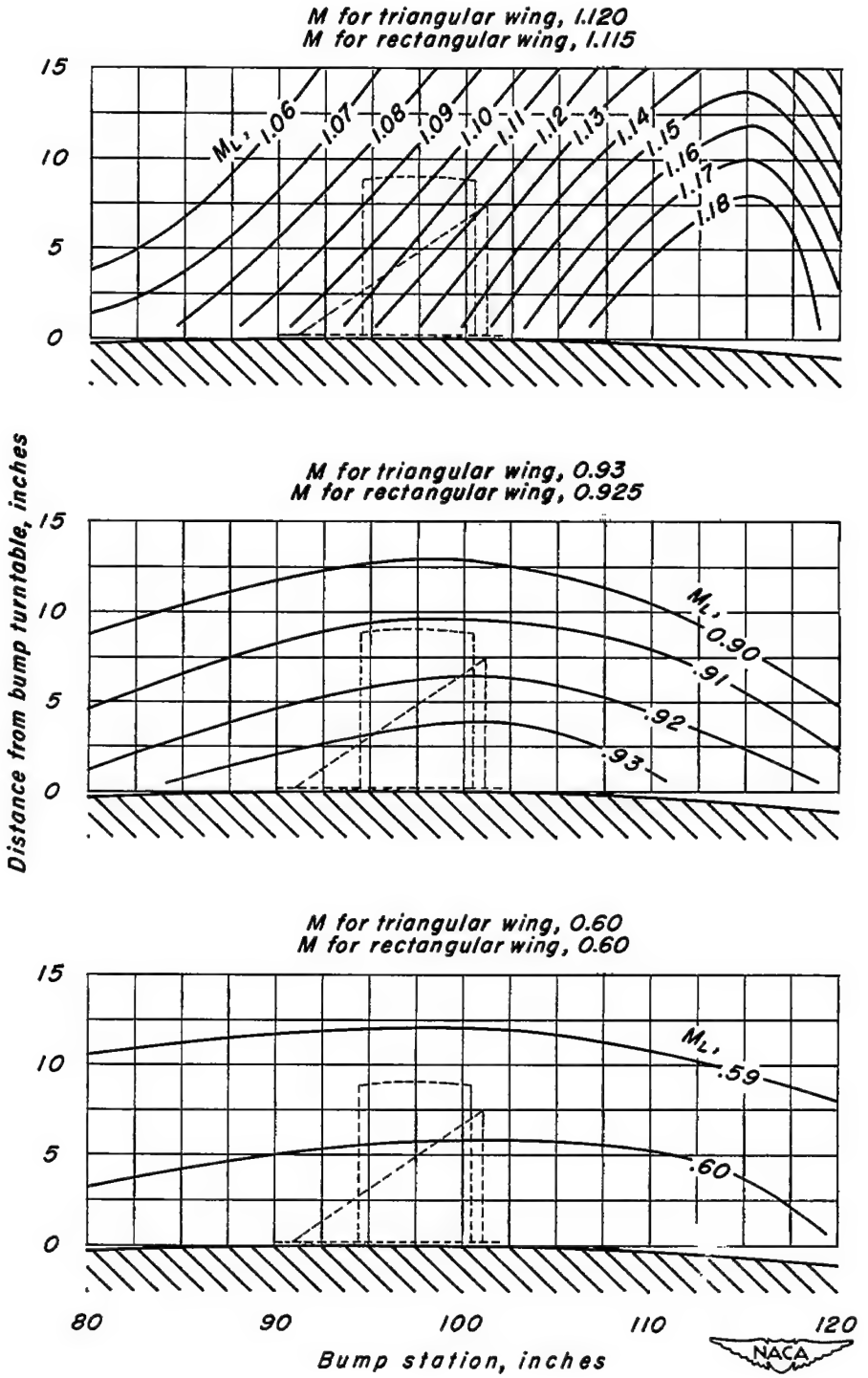

Figure 4.- Typical Mach number contours over the transonic bump in the Ames 16-foot high-speed wind tunnel.

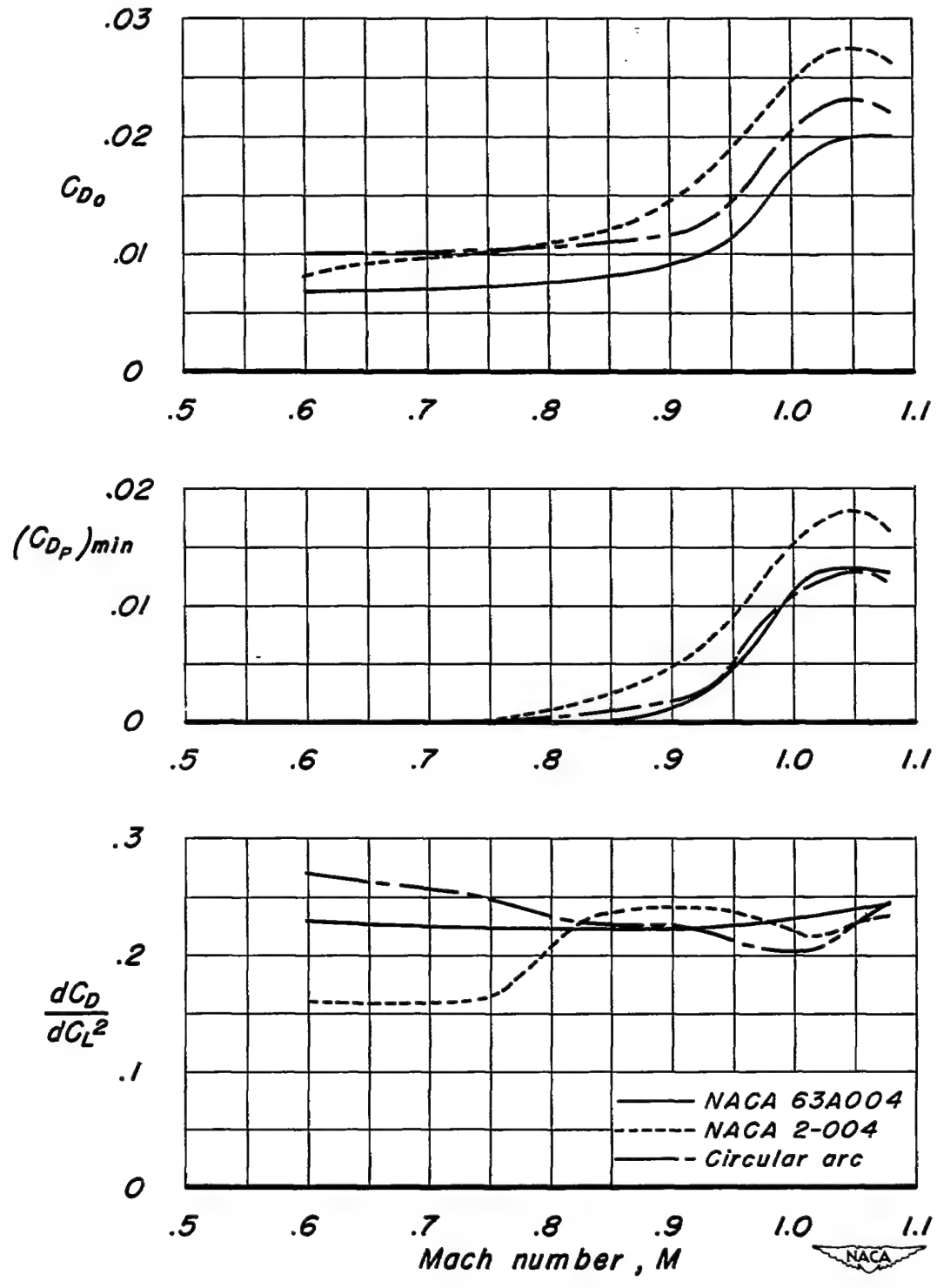

Figure 5.- Summary of the drag characteristics of the rectangular wings.

[redacted]

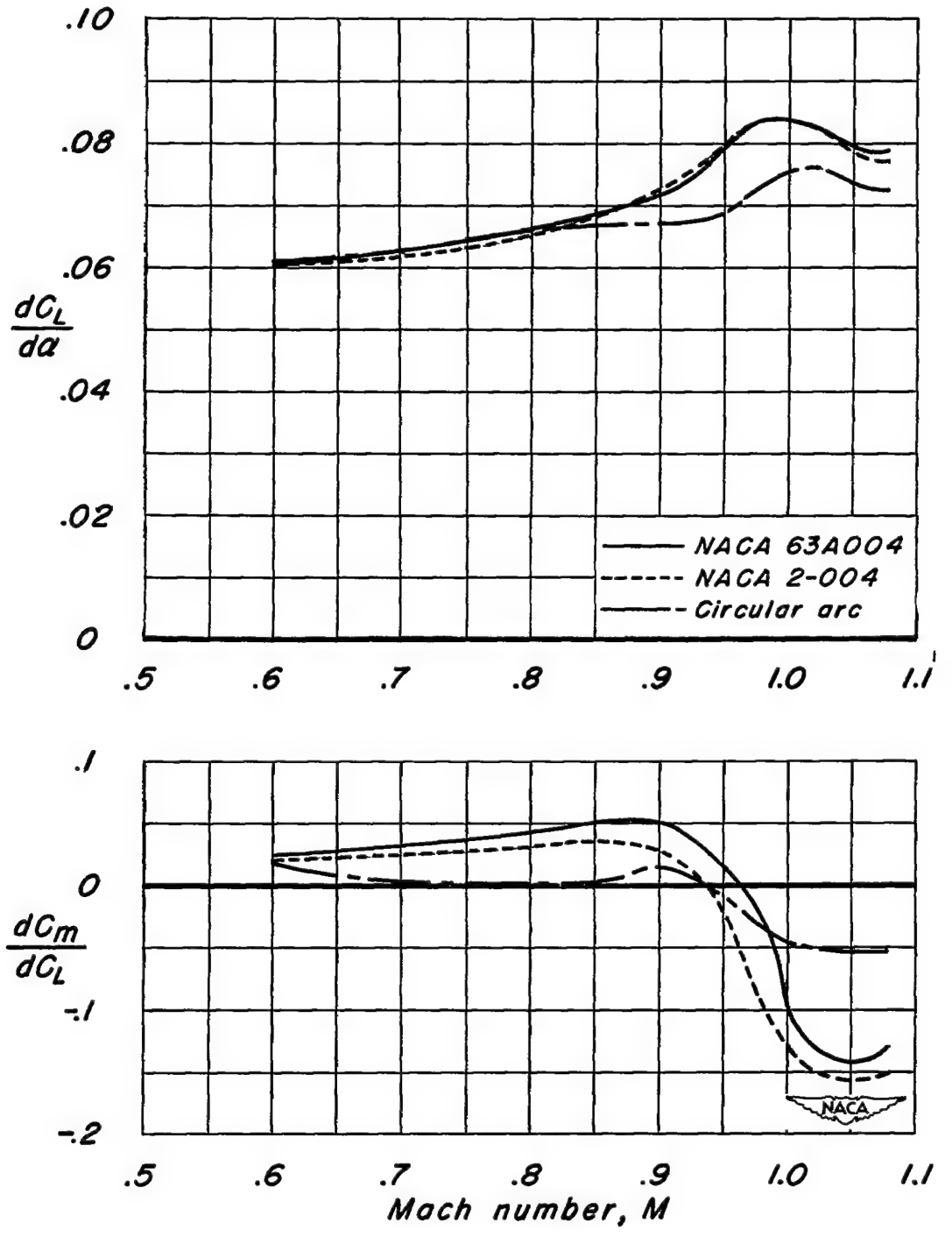

Figure 6.- Slopes of the lift and pitching-moment characteristics of the rectangular wings.

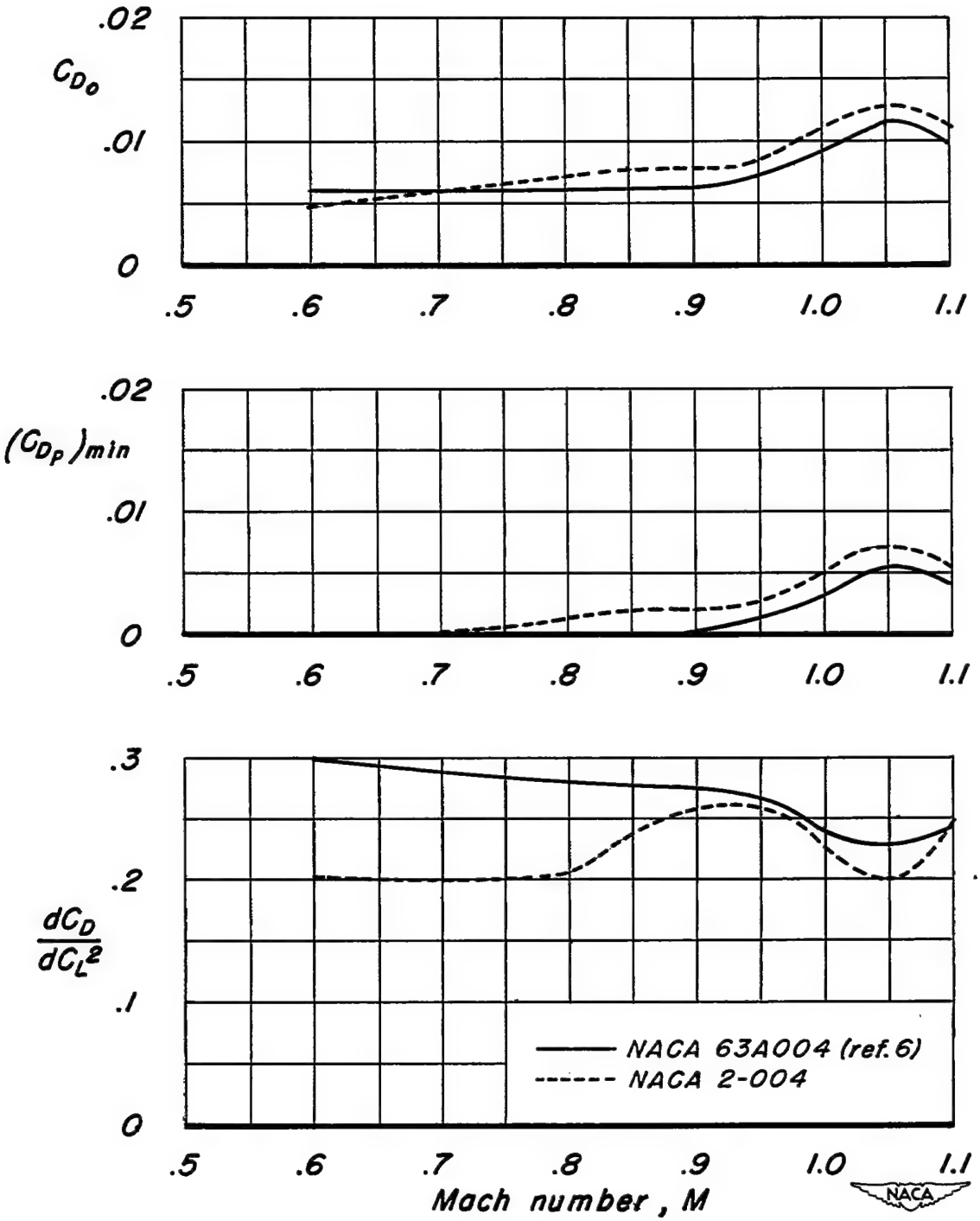

Figure 7.- Summary of the drag characteristics of the triangular wings.

[redacted]

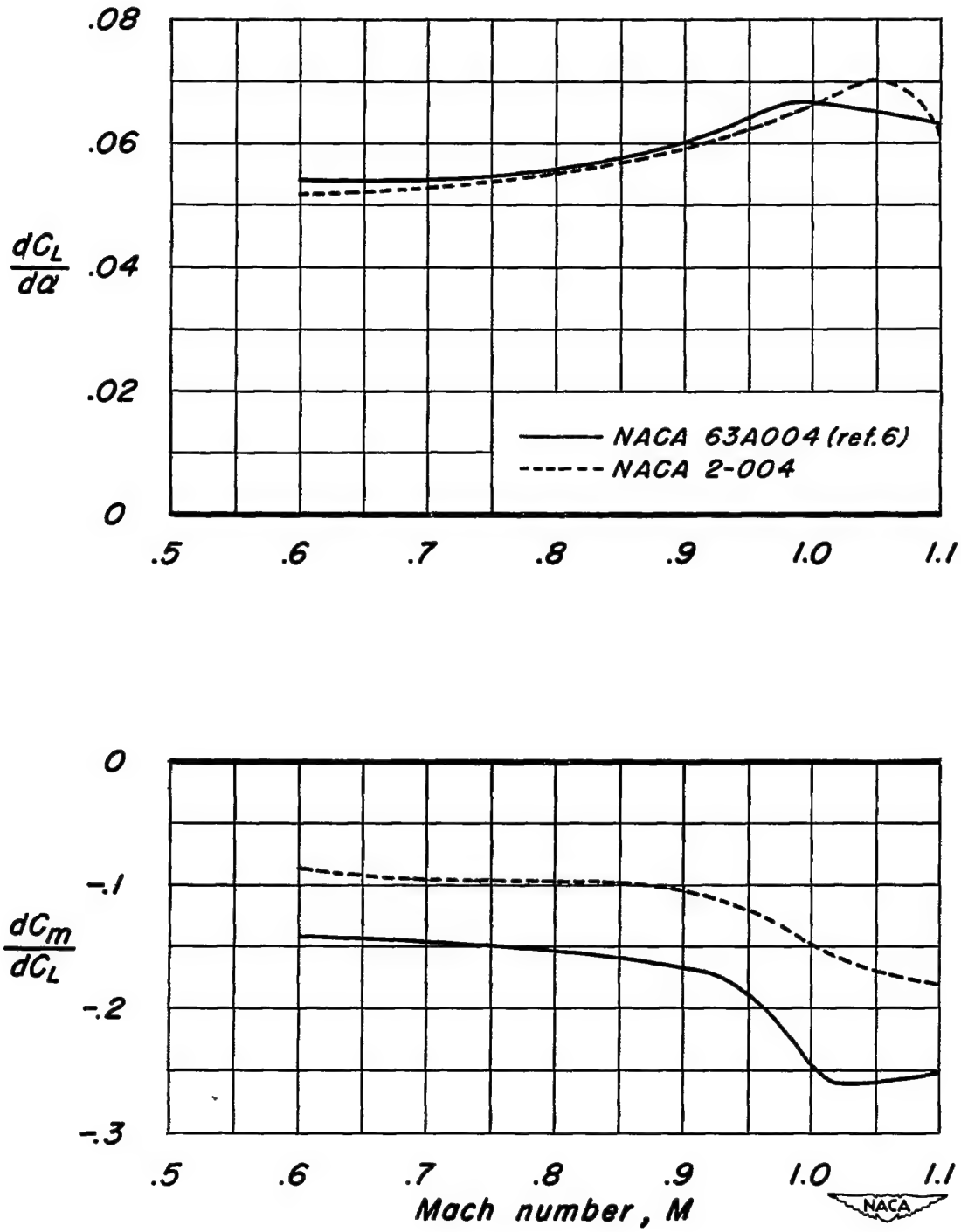

Figure 8.- Slopes of the lift and pitching-moment characteristics of the triangular wings.

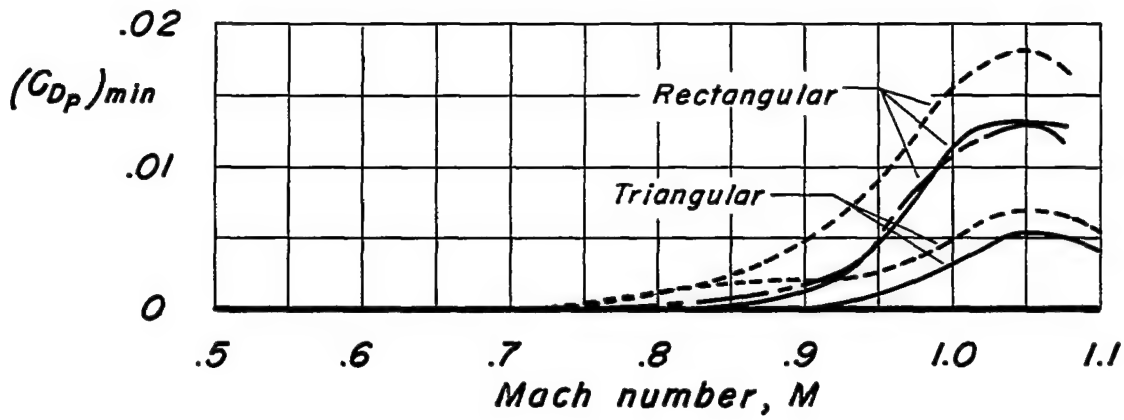

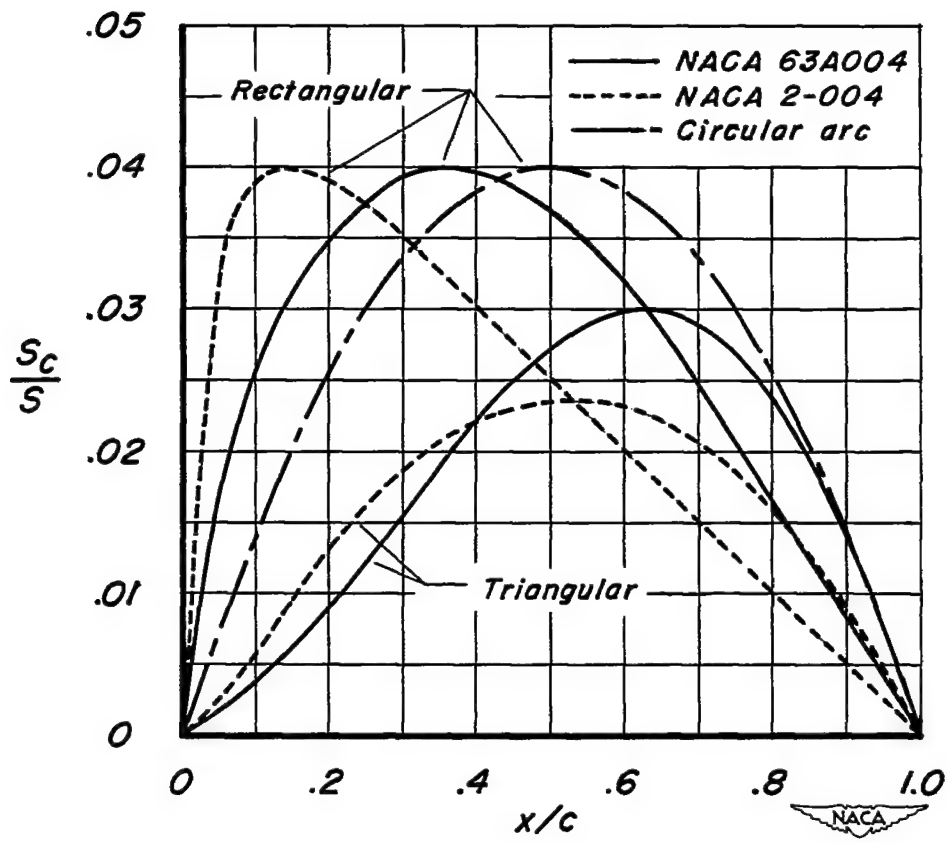

Figure 9.- Chordwise distribution of cross-sectional areas, and minimum pressure-drag coefficients for the wings.

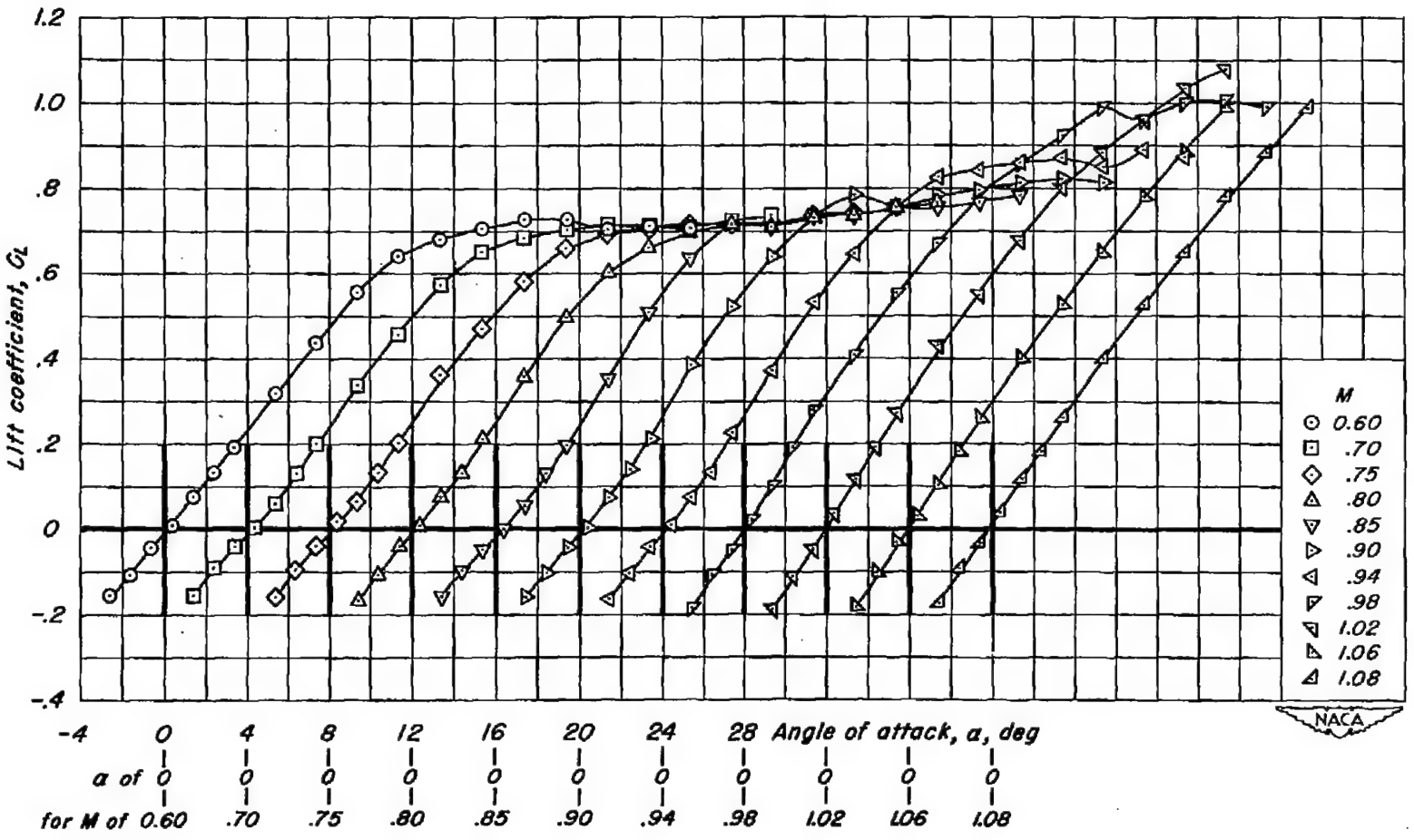

(a) C_L vs. α

Figure 10.- Lift, drag, and pitching-moment characteristics of the rectangular wing having a circular-arc profile.

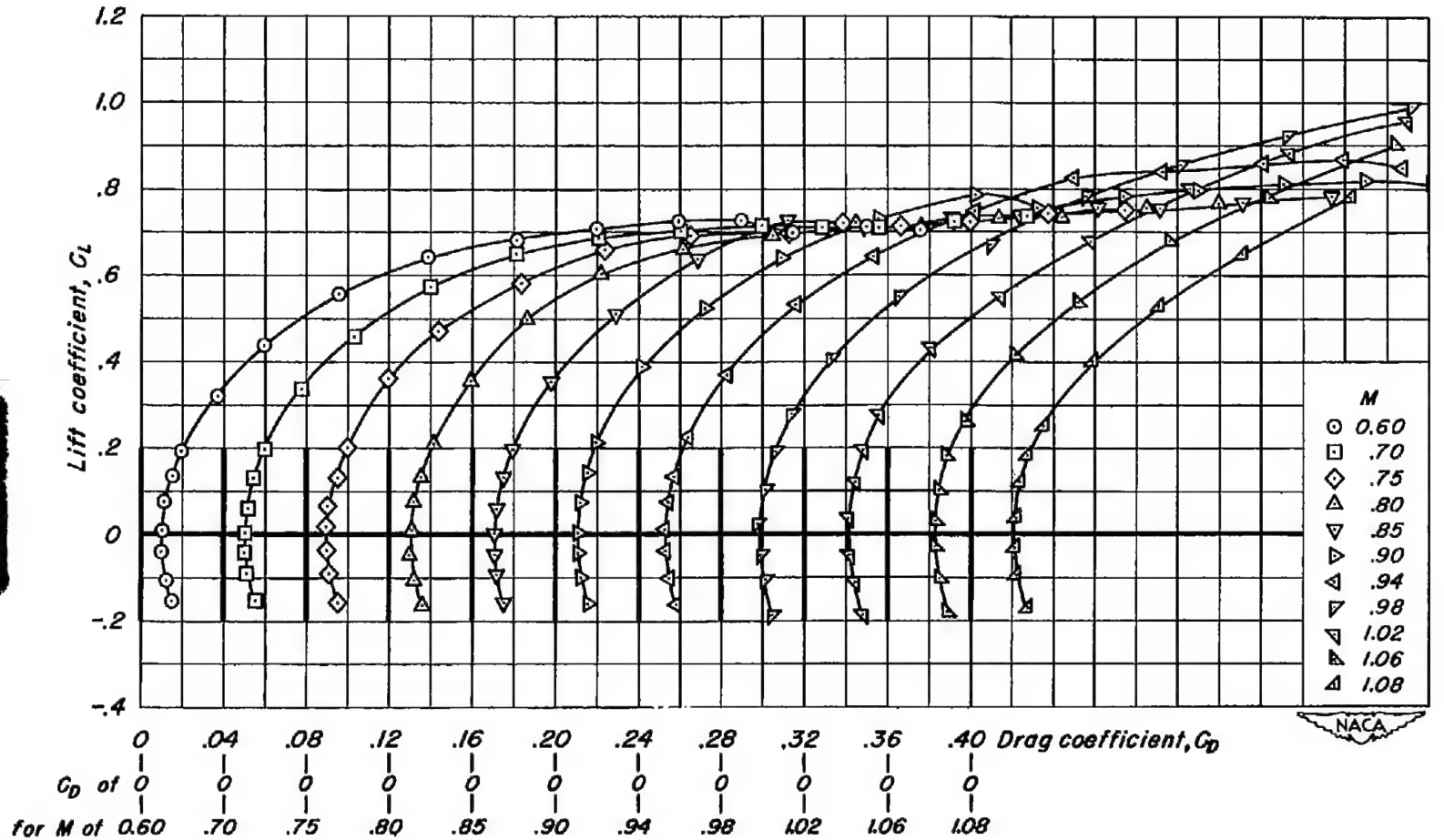

(b) C_L vs. C_D

Figure 10.- Continued.

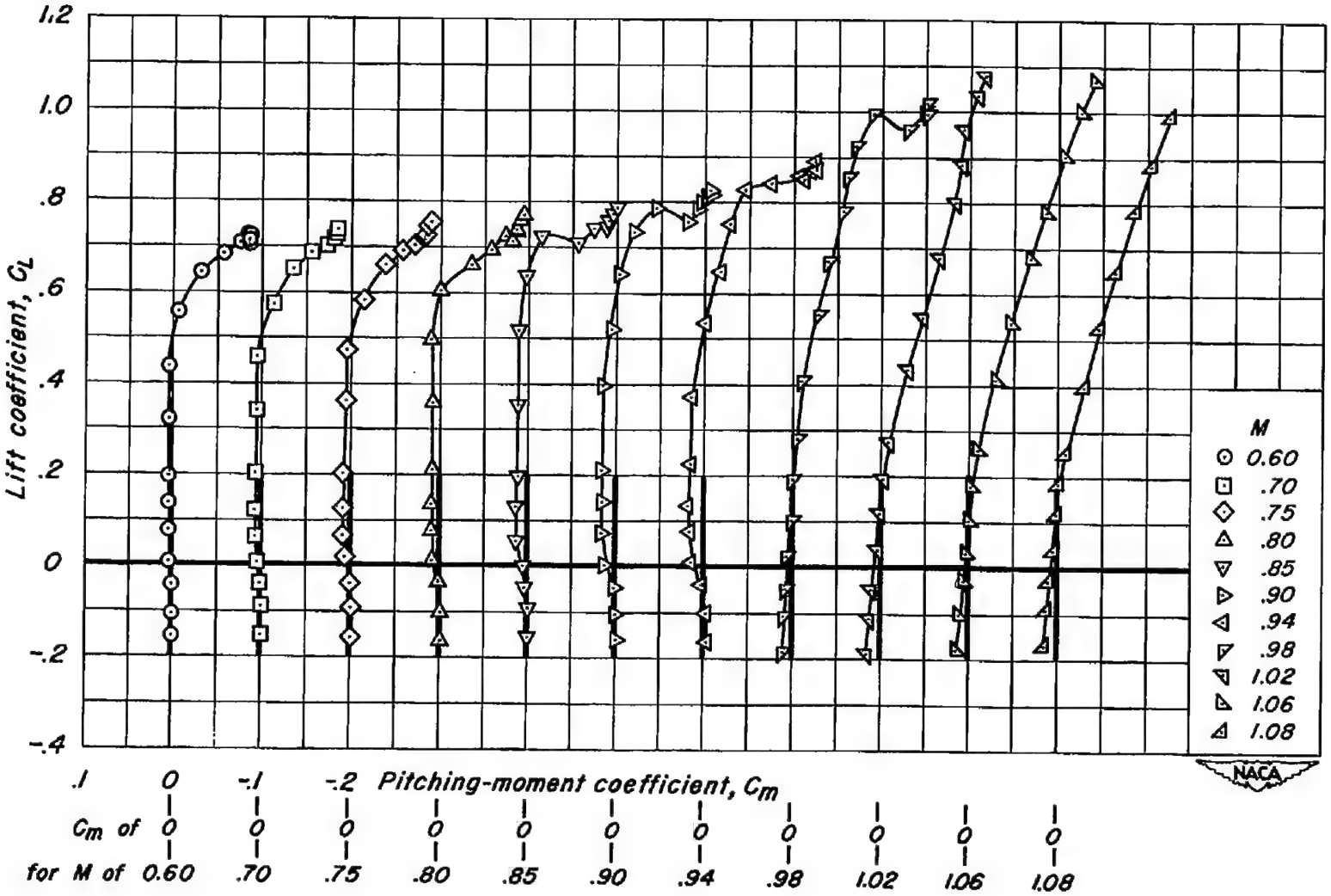

(c) C_L vs. C_m

Figure 10.- Concluded.

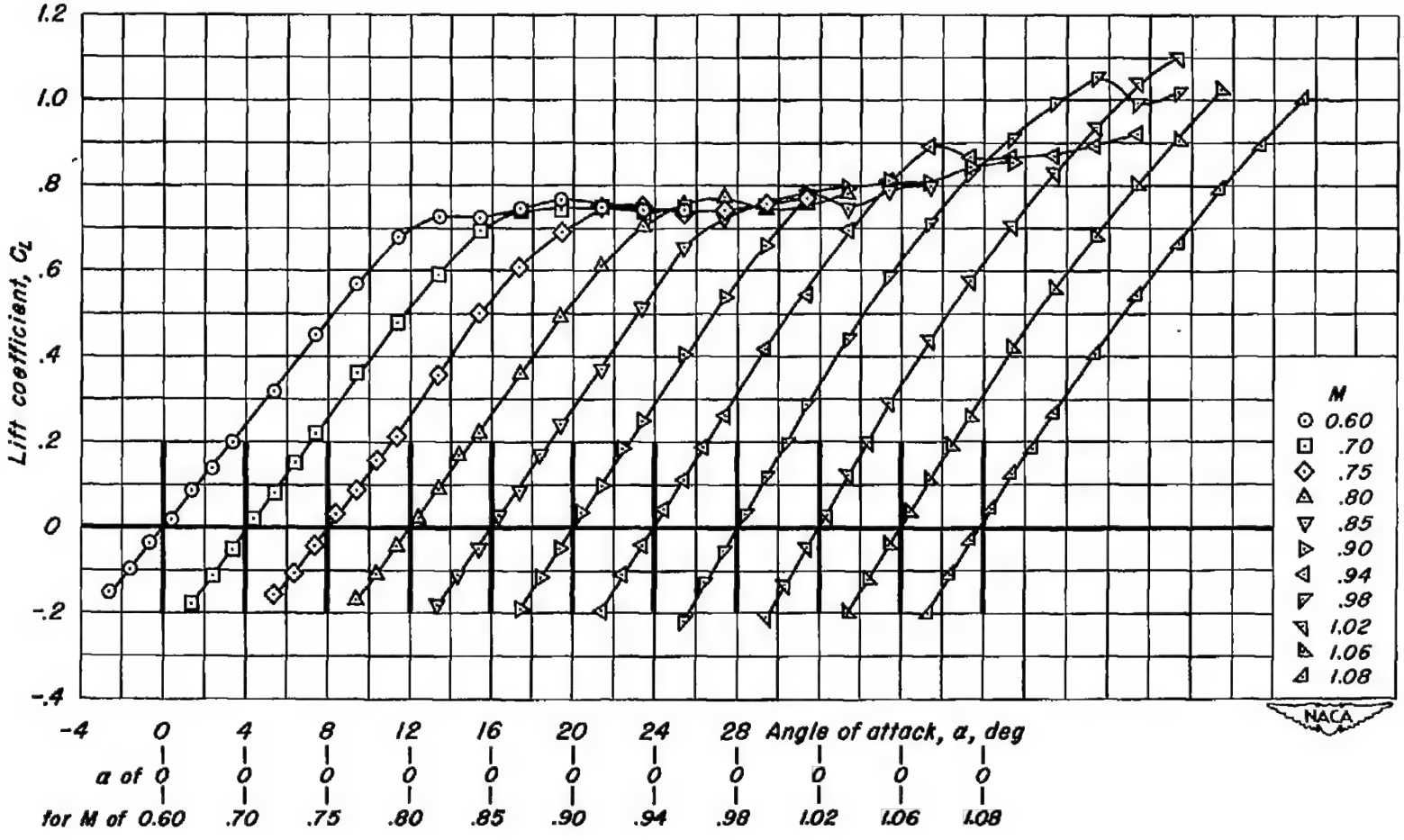

(a) C_L vs. α

Figure 11.- Lift, drag, and pitching-moment characteristics of the rectangular wing having an NACA 2-004 profile.

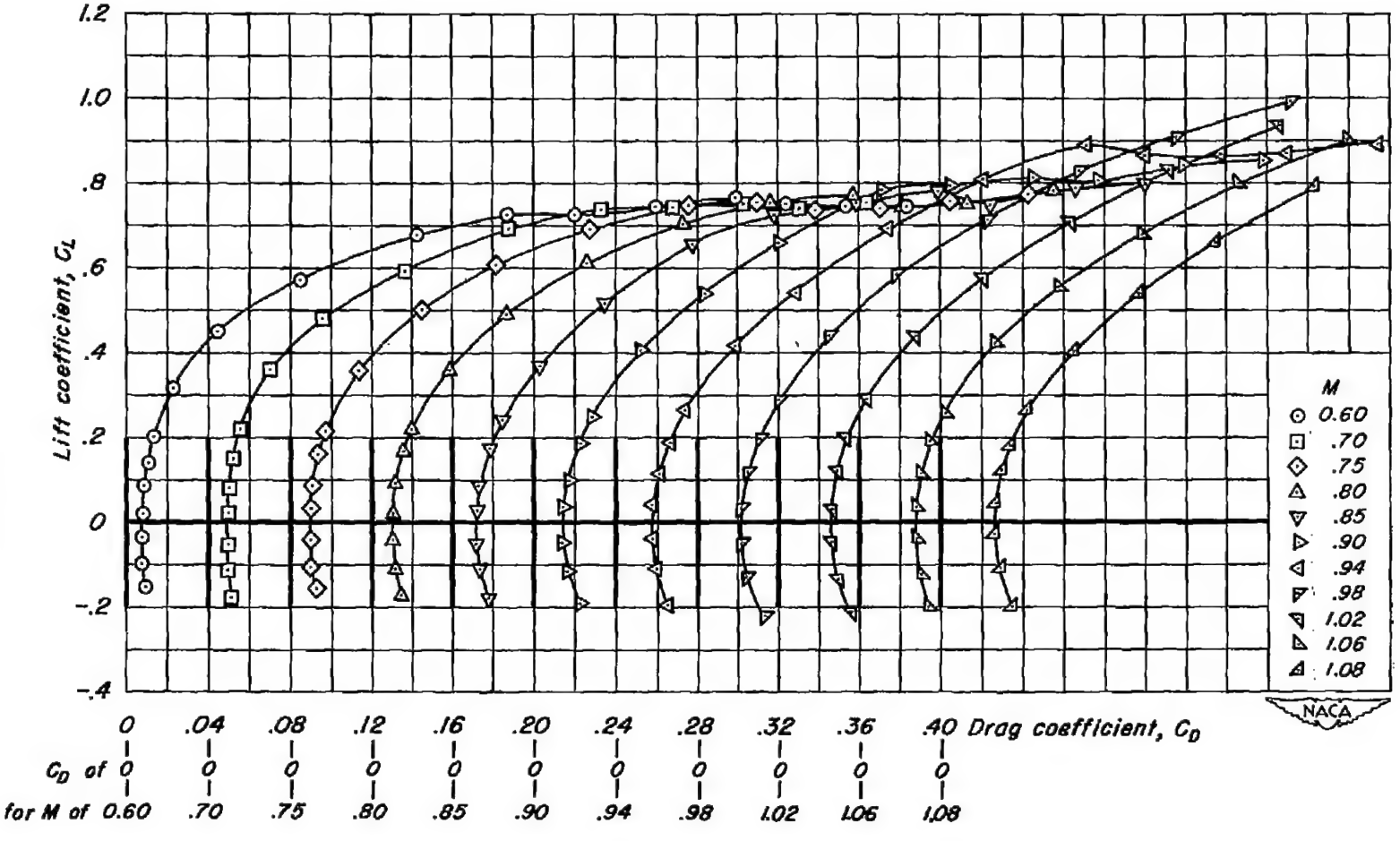

(b) C_L vs. C_D

Figure 11.- Continued.

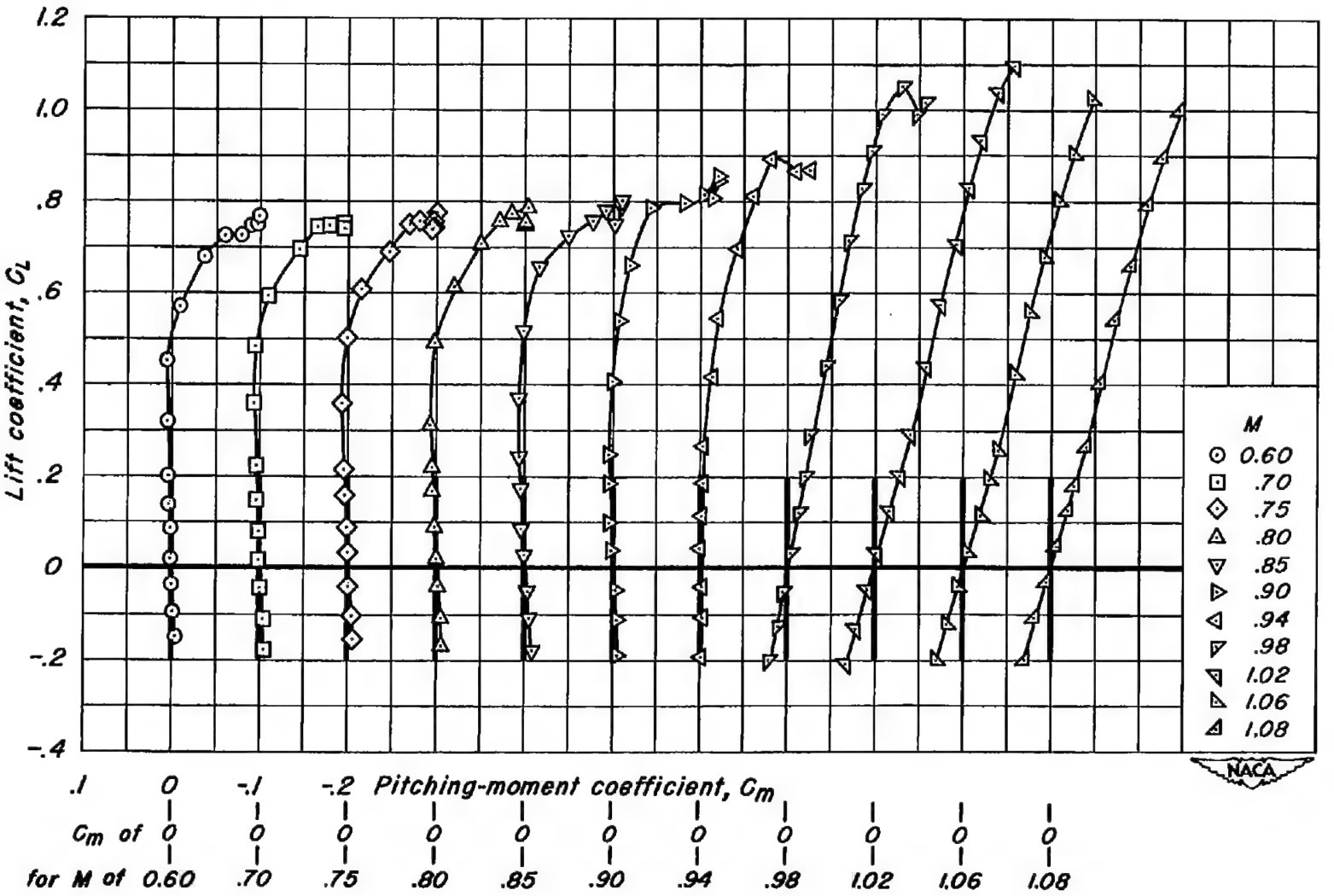

(c) C_L vs. C_m

Figure 11.- Concluded.

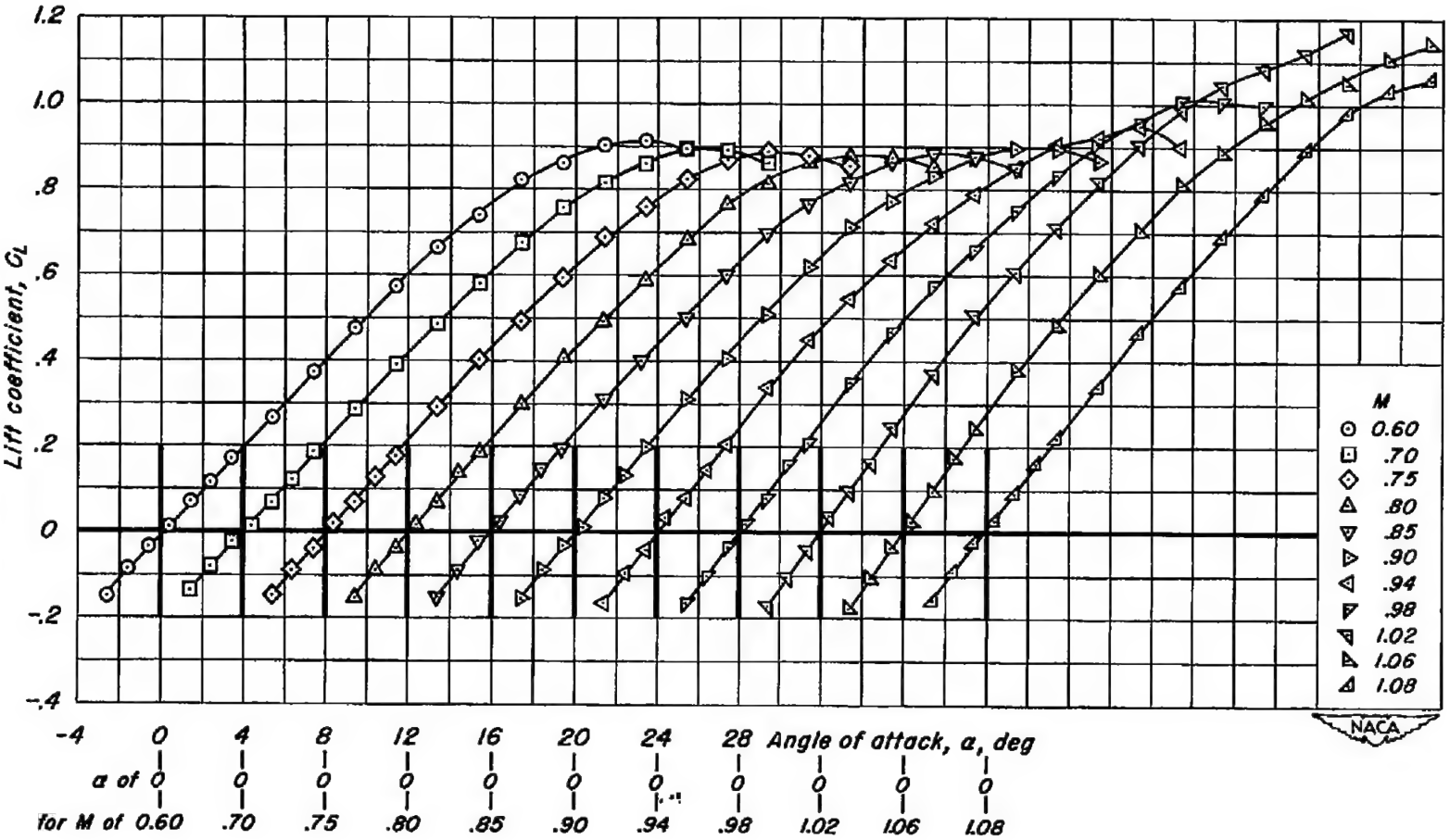

(a) C_L vs. α

Figure 12.- Lift, drag, and pitching-moment characteristics of the triangular wing having an NACA 2-004 profile.

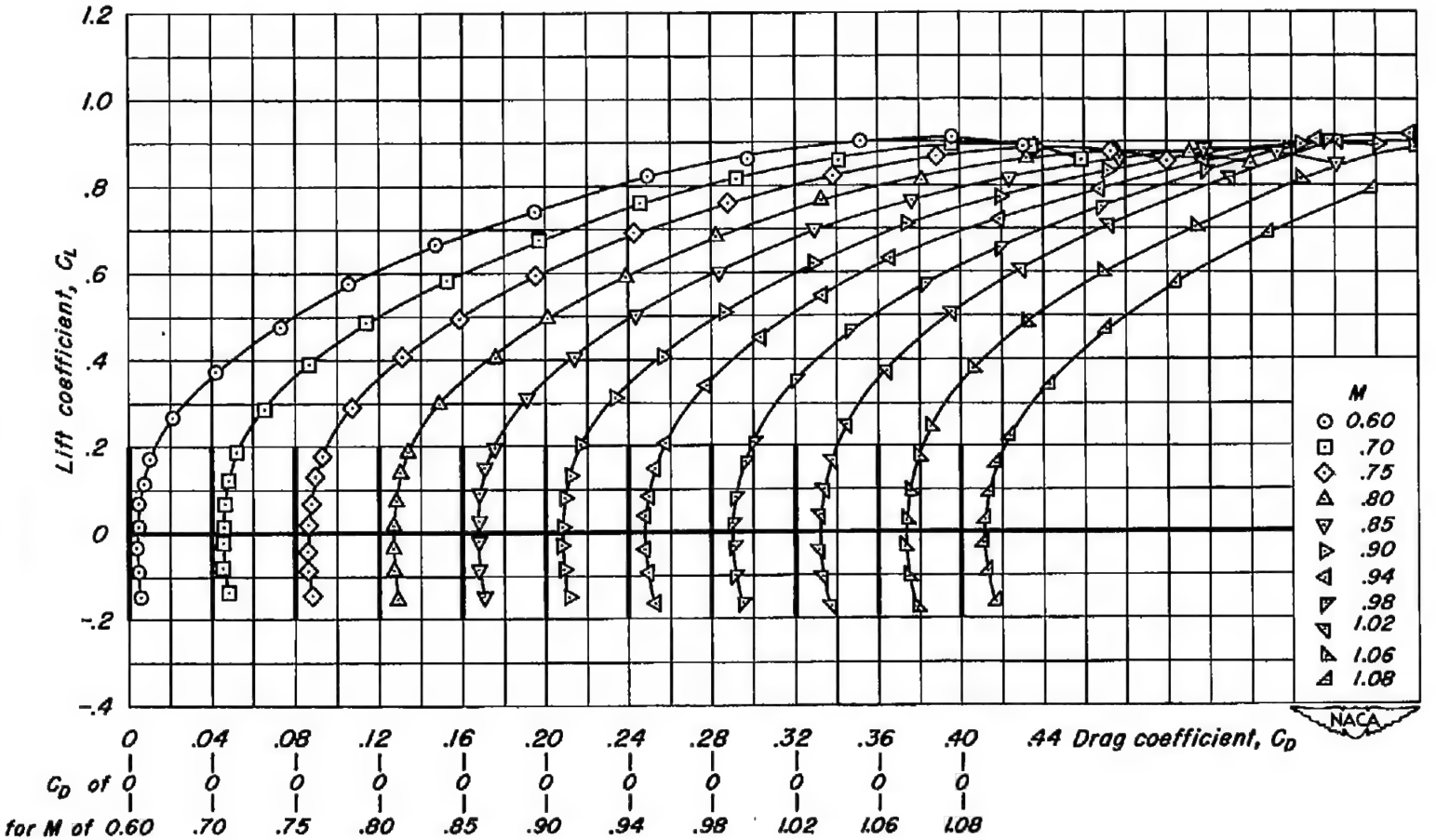

(b) C_L vs. C_D

Figure 12.- Continued.

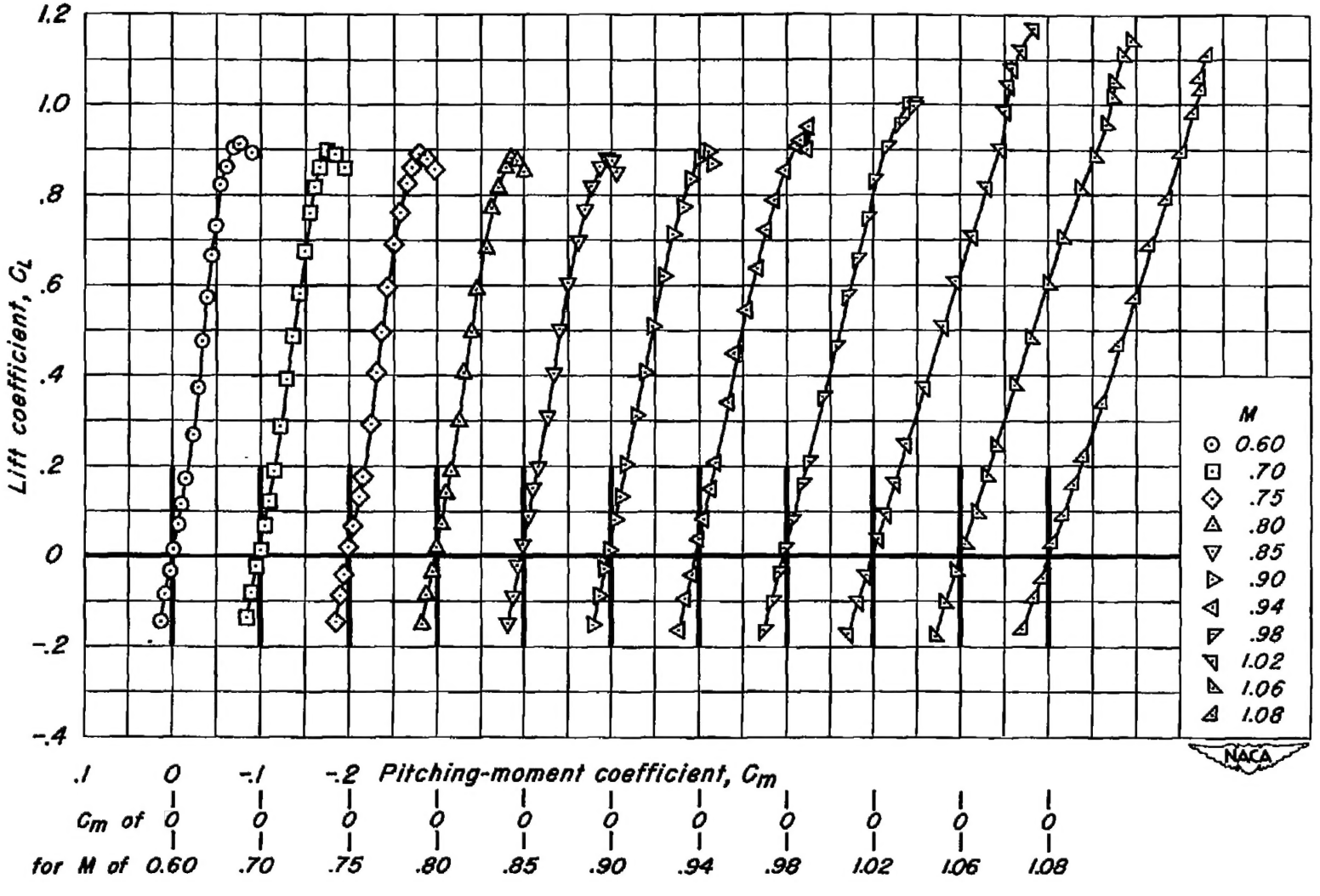

(c) C_L vs. C_m

Figure 12.- Concluded.

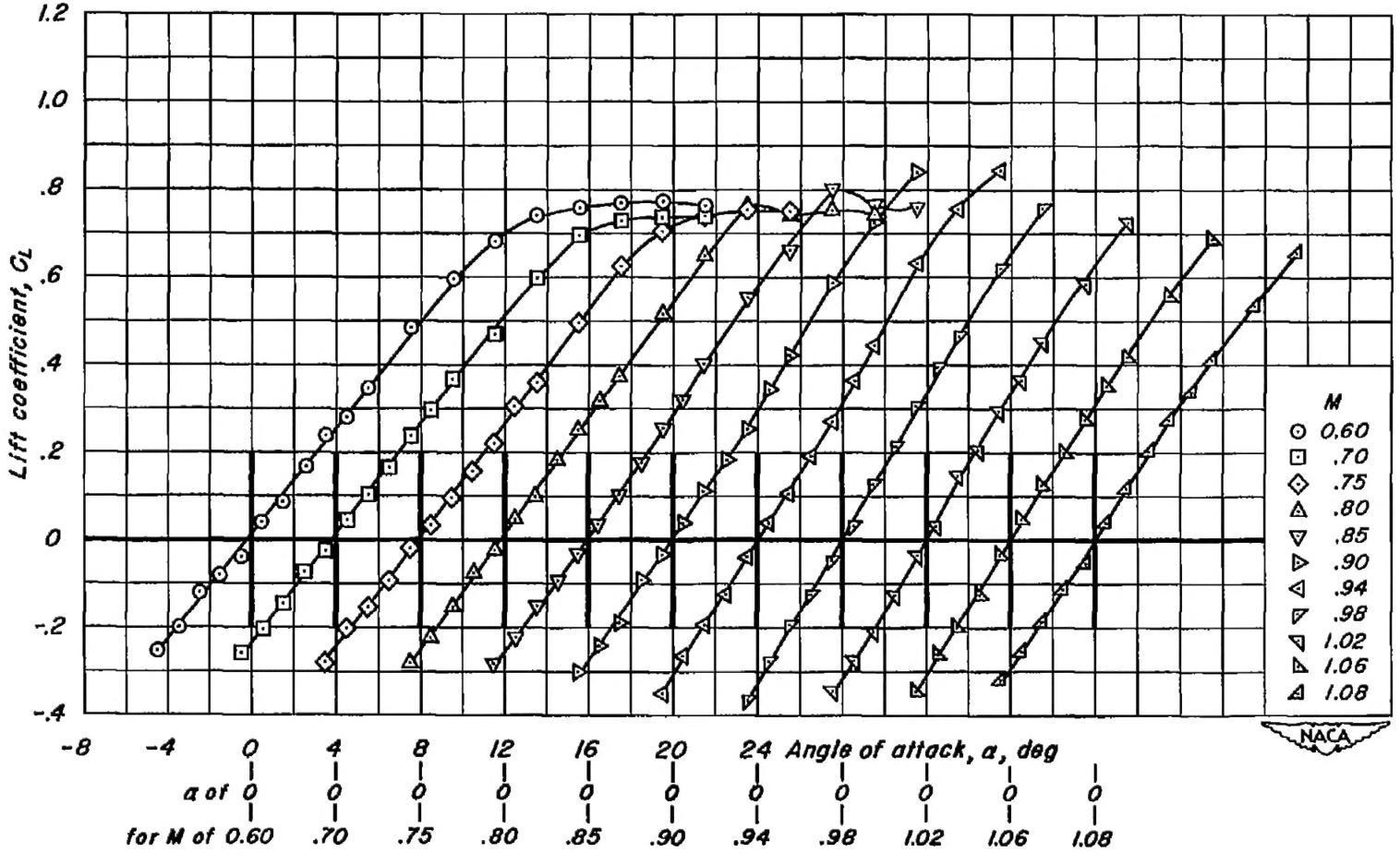

(a) C_L vs. α

Figure 13.- Lift, drag, and pitching-moment characteristics of the rectangular wing having an NACA 63A004 profile.

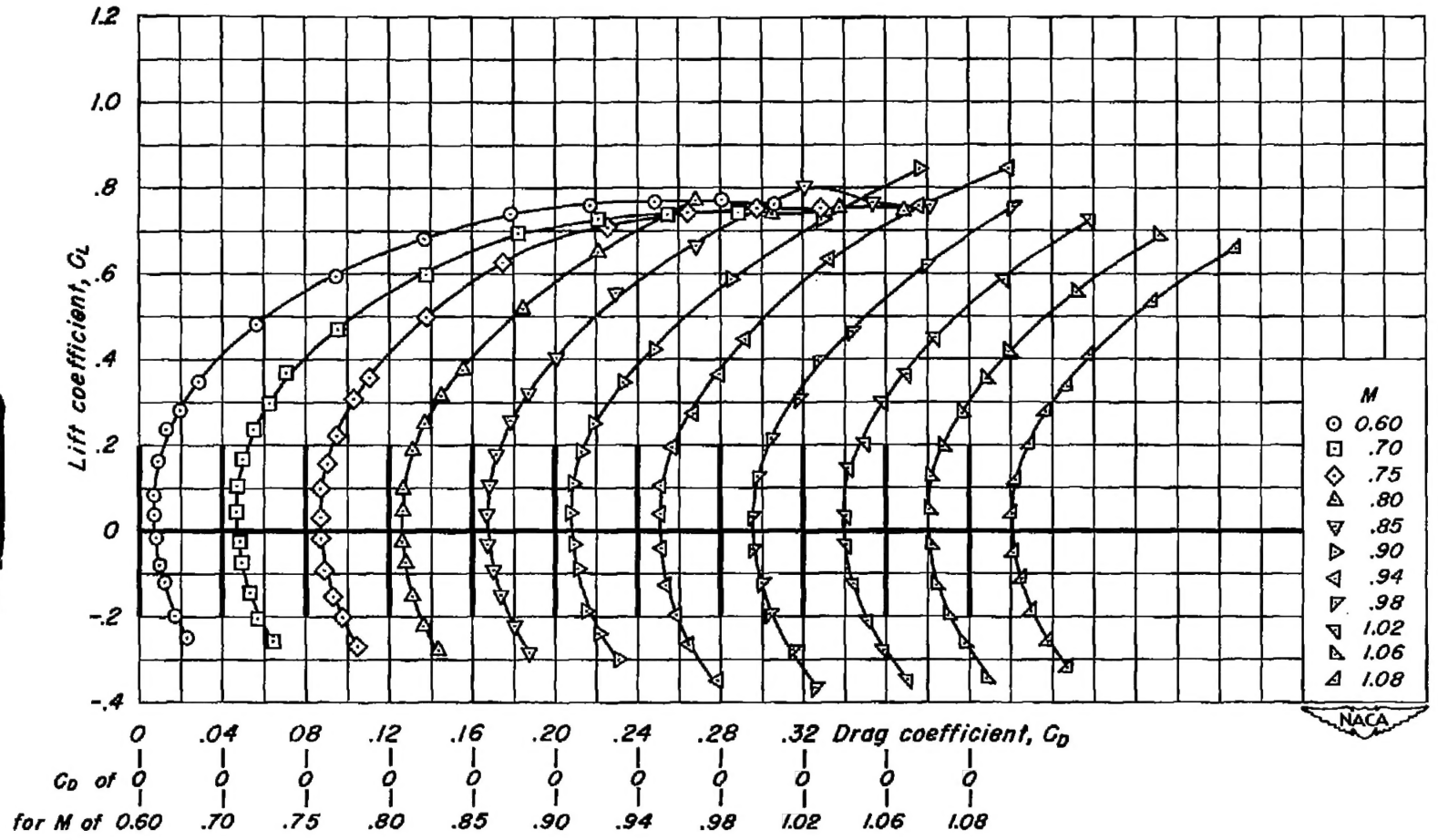

(b) C_L vs. C_D

Figure 13.- Continued.

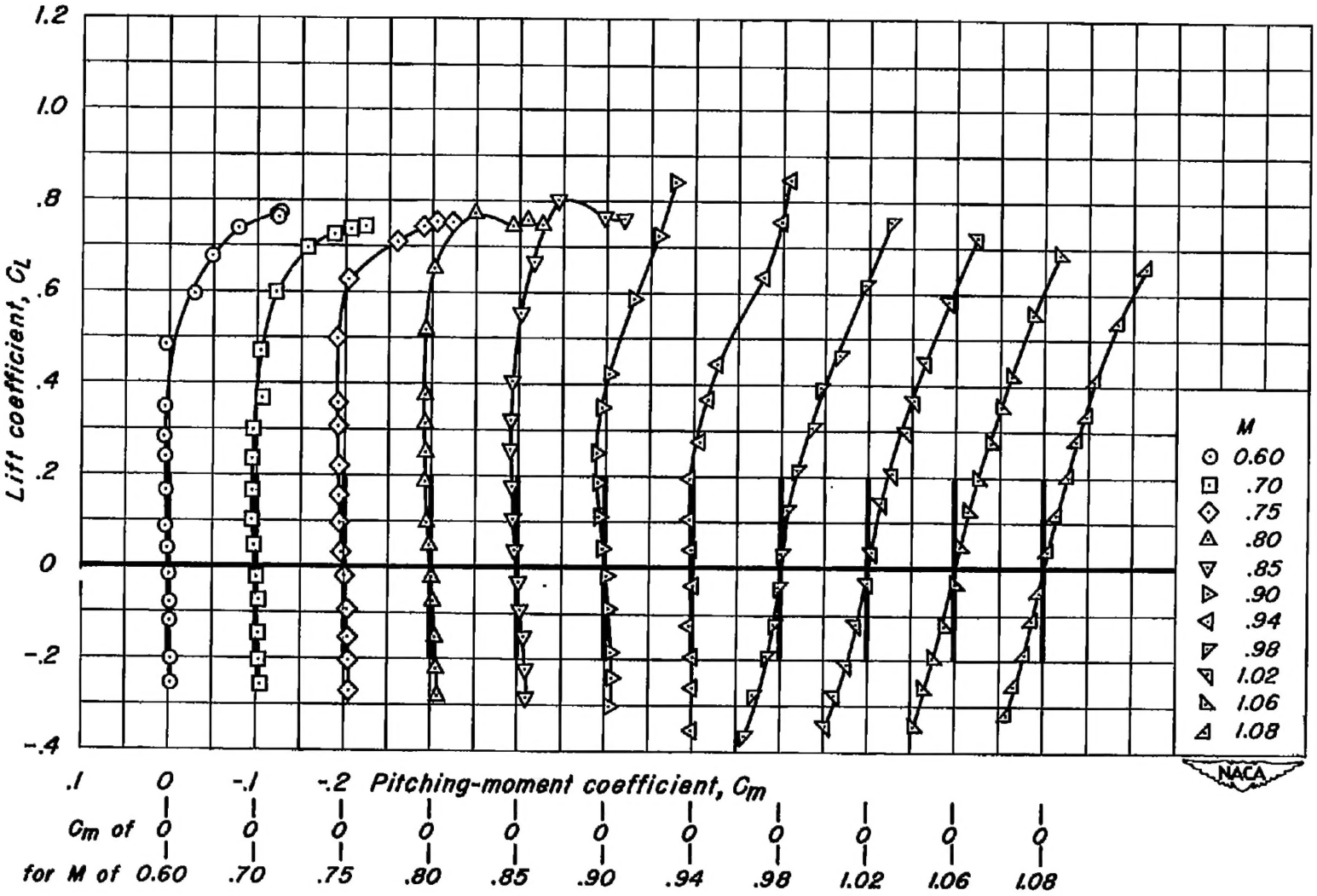

(c) C_L vs. C_m

Figure 13.- Concluded.